Validation of a spatial-temporal soil water movement and plant water uptake model

J. Heppell[1,3,4,5*], S. Payvandi[2,4], K. C. Zygalakis[3,4,5], J. Smethurst[2], J. Fliege[3,5] and T. Roose[2,4]

[1] Institute for complex systems simulation, University of Southampton [2] Faculty of Engineering and the Environment, University of Southampton [3] CORMSIS, University of Southampton [4] IFLS Crop Systems Engineering, University of Southampton [5] School of Mathematics, University of Southampton

*Corresponding author: E-mail address: jph106@soton.ac.uk (James Heppell).

S.Payvandi@soton.ac.uk , K.Zygalakis@soton.ac.uk , J.A.SMETHURST@soton.ac.uk , J.Fliege@soton.ac.uk , T.Roose@soton.ac.uk

Abstract

Management and irrigation of plants increasingly relies on accurate mathematical models for the movement of water within unsaturated soils. Current models often use values for water content and soil parameters that are averaged over the soil profile. However, many applications require models to more accurately represent the soil-plant-atmosphere continuum, in particular, water movement and saturation within specific parts of the soil profile. In this paper a mathematical model for water uptake by a plant root system from unsaturated soil is presented. The model provides an estimate of the water content level within the soil at different depths, and the uptake of water by the root system. The model was validated using field data, which includes hourly water content values at five different soil depths under a grass/herb cover over one year, to obtain a fully calibrated system for plant water uptake with respect to climate conditions. When compared quantitatively to a simple water balance model, the proposed model achieves a better fit to the experimental data due to its

ability to vary water content with depth. To accurately model the water content in the soil profile, the soil water retention curve and saturated hydraulic conductivity needed to vary with depth.

1. Introduction

In the UK, shrink and swell displacements caused by seasonal changes in clay soil water content can cause serviceability problems for vegetated earthworks (Andrei, 2000; O'Brien, 2007) and exacerbate the progressive failure of clay slopes (Vaughan et al, 2004). Clay shrinkage in dry summers also regularly causes damage to older buildings constructed on shallow foundations (Driscoll, 1983).

With the onset of global warming, weather systems and in particular rainfall patterns are likely to change. This climatic change will have an impact on plants that interact with engineered structures such as earthworks and shallow foundations (Clarke and Smethurst, 2010). In order to optimize soil-water and plant management strategies it is necessary to understand current plant-soil systems and their reactions to varying rainfall and climate patterns.

A number of agronomic models exist that calculate changes in water content within the soil in response to climate and plant water uptake. However, many of these models only estimate the average water saturation level within the plant root zone. Common examples used in agriculture (and to some extent, in engineering, e.g. Clarke and Smethurst, 2010) include DASSAT (Jones et al, 2003), APSIM (McCown et al, 1996) and CROPWAT (Clarke et al, 1998).

CROPWAT carries out a water balance calculation for the rooting zone, determining an average soil saturation which varies in response to rainfall infiltration and plant evapotranspiration, calculated using the Penman-Monteith equation (Allen et al, 1994). Many of these models are adequate for simple crop management and irrigation purposes. However, applications in engineering and agricultural sciences need models to more accurately represent the soil-plant-atmosphere continuum, in particular the water movement and content within specific parts of the soil profile. In

engineering, the stability of many embankments and cut slopes is dependent on the presence of soil suctions both within and below the rooting zone, and more advanced models are needed to investigate vegetation management options (Loveridge et al, 2010; Briggs et al, 2013).

A difficulty with trying to model the water content levels at different soil depths is the characterisation of the parameters that control the soil water content and flow processes. Both soil water retention and permeability can be difficult to measure accurately, and there is often little or no site specific data, yet modelling responses can be very sensitive to these parameters (Rahardjo et al, 2001; Rouainia et al, 2009; Nyambayo and Potts, 2010; Smethurst et al, 2012). Data on root structures and temporal soil and plant interactions with time can also be sparse. However, there are often good records for water content and climate conditions, which can be used to calibrate models.

This paper develops a computational approach to calculate the water content at different depths in the soil based on an extension of the model for water flow and plant water uptake given by Roose and Fowler (2004). Environmental inputs are added which estimate the water flux into the soil and root internal pressure. This model is validated against climate and water content data measured by Smethurst et al (2012) at a site in Newbury. A numerical procedure is then used to optimise the model input parameters and distributions of some of the more uncertain soil parameters (such as soil permeability, soil-water retention, and root density) to obtain a best fit to the measured water content data. The model is spatially explicit, allowing the distribution of water within the soil profile to be determined.

2. Field data

The field data used to calibrate the numerical model have been taken from instrumentation installed into a cut slope adjacent to the A34 Newbury bypass in England (Ordnance Survey grid reference SU455652). The site, and the full range of instrumentation installed, is described in detail in

Smethurst et al (2006, 2012). The 16 degree, 8 m high slope is cut entirely within London Clay, which is weathered over a depth of about 2.5 to 3.0 m below the original ground level (Fig. 1).

The vegetation cover is primarily rough grass with herbs, with some small shrubs mainly of Hazel, which towards the start of the study (the data used are from 2005) were generally less than 0.5 m high. Recent observations made from shallow vertical faces cut into the slope indicate that the roots extend to about 0.8 m depth. Although detailed root density measurements were not taken in 2005, the plants had been growing on the slope for over 6 years, and therefore were well established.

Time domain reflectrometry (TDR) probes were installed at depths of 0.3, 0.45, 0.6, 0.9 and 1.5 m at different locations (A and C; Fig. 1) on the slope, to record volumetric soil water content (units of m^3 of water per m^3 of soil) every hour. A climate station was installed at the site to measure rainfall, air temperature, humidity, wind speed and solar radiation. Surface runoff and interflow (flow of water through the topsoil) were measured using an interceptor drain cut to 0.35 m depth across the face of the slope. Soil pore water pressures (or suctions) were also recorded every hour, as described in Smethurst et al (2012).

3. Model

3.1 Water movement and plant water uptake model

Roose and Fowler (2004) developed a model describing the movement of water within an unsaturated soil surrounding a root. The model provides an estimate of the soil water content at different depths, and the uptake of water by the root system. The important aspects of the model are presented here; full details are given in Roose and Fowler (2004).

A one year data set (2005) collected from Smethurst et al (2012) was used to validate the Roose and Fowler (2004) model, which included determining optimal values of some root and soil water parameters. These were then used within the model with further climate data to see if the optimised model was able to produce predictions of changes in water content comparable with

those measured in later years. A number of changes were made to the Roose and Fowler (2004) model to allow it to link with climate parameters such as rainfall, air temperature, wind speed and humidity and hence to the measured data; these changes are discussed below.

The model is based on the equation for the conservation of water in the soil (Richards equation), which is given by:

$$\theta_s \frac{\partial S}{\partial t} + \boldsymbol{\nabla} \cdot \boldsymbol{u} = -F_W, \tag{1}$$

where S is the relative water saturation in the soil ($S = (\theta - \theta_r)/(\theta_s - \theta_r)$, where θ is the volumetric water content, θ_s is soil porosity and θ_r is the residual water content; S also denotes the normalized volumetric water content, with the Eurocode 7 descriptor Θ), $\boldsymbol{u}$ is the volume flux of water ($m\ s^{-1}$) and F_W is the uptake of water by the plant roots (volume per unit time per unit volume of soil). The residual water content θ_r was taken as zero since at very high suctions in clay soils it does become close to zero (Croney, 1977; Fig. 2). The volume flux of water is represented by Darcy's law,

$$\boldsymbol{u} = -\frac{k}{\mu}\left[\boldsymbol{\nabla} p - \rho g \widehat{\boldsymbol{k}}\right], \tag{2}$$

where k is the soil permeability (m^2), p is the water pressure in the soil (Pa), μ is the dynamic viscosity of water ($kg\ s^{-1}m^{-1}$), ρ is the density of water ($kg\ m^{-3}$), g is the gravitational acceleration ($m\ s^{-2}$) and $\widehat{\boldsymbol{k}}$ is the unit vector in the downward direction.

It is also possible to write the water pressure in the partially saturated soil pores in terms of the relative saturation via the soil water retention curve (Van Genuchten, 1980),

$$p_a - p = p_c f(S), \quad f(S) = (S^{-1/m} - 1)^{1-m} \quad , \tag{3}$$

where p_a (Pa) is the atmospheric pressure, p_c (Pa) is a characteristic suction pressure determined from experimental data for different types of soil and m denotes the Van Genuchten soil suction parameter, where $0 < m < 1$. Measuring gauge pressures relative to atmospheric pressure gives $p_a = 0$.

Soil permeability is influenced by soil saturation, and therefore the soil permeability is written in terms of relative water content using Van Genuchten (1980),

$$k = k_s K(S) = k_s S^{1/2}\left[1 - \left(1 - S^{1/m}\right)^m\right]^2, \tag{4}$$

where k_s is the water permeability in fully saturated soil (m^2), and $K(S)$ represents the reduction in water mobility in the soil due to the reduction in relative saturation. The air entry value (the soil suction at which the volumetric water content reduces from full saturation) is represented in the Van Genuchten expression (Equation 3) by a combination of m and p_c. It is most sensitive to p_c and decreases as $p_c$decreases (Fig. 2).

The water uptake by a single cylindrical root is calculated from the difference between soil pore water pressure and root xylem pressure (the water pressure in the root), and is given by

$$F_W = 2\pi a l_d k_r (p - p_r) = 2\pi a l_d k_r (-p_c f(S) - p_r), \tag{5}$$

where $2\pi a l_d$ is the root surface area density, l_d is the root length density (m of roots per $m^3$of soil), a is the average root radius (m), k_r is the root radial water conductivity parameter $(m\ s^{-1}\ Pa^{-1})$ and p_r is the root internal xylem pressure (Pa).

Using equations (3) and (4), we can write equation (1) in terms of the relative saturation S only,

$$\theta_s \frac{\partial S}{\partial t} = \boldsymbol{\nabla} \cdot \left[D_0 D(S) \boldsymbol{\nabla} S - K_s K(S) \hat{\boldsymbol{k}} \right] - F_W, \tag{6}$$

where the water "diffusivity" in the soil is $D_0 D(S) = (k/\mu) \left| \frac{\partial p}{\partial S} \right|$,

$$D_0 = \frac{p_c k_s}{\mu} \left(\frac{1-m}{m} \right), \tag{7}$$

$$D(S) = S^{\frac{1}{2} - \frac{1}{m}} \left[\left(1 - S^{\frac{1}{m}} \right)^{-m} + \left(1 - S^{\frac{1}{m}} \right)^{m} - 2 \right], \tag{8}$$

and K_s is the saturated hydraulic conductivity ($m\ s^{-1}$) given by,

$$K_s = \frac{\rho g k_s}{\mu}. \tag{9}$$

The boundary conditions for the model are

$$D_0 D(S) \frac{\partial S}{\partial x} - K_s K(S) = \begin{cases} -W & at \quad x=0 \\ 0 & at \quad x=l_w \end{cases}, \tag{10}$$

where W is the volume flux of water into the soil at the surface, representing both infiltration due to precipitation and evaporation (volume of water per unit soil surface area per unit time), and l_w is the depth at which zero water flux occurs.

The balance between the axial and radial fluxes of water inside a single cylindrical root is given by

$$2\pi a k_r(-p_c f(S) - p_r) = -k_z \frac{\partial^2 p_r}{\partial x^2}, \tag{11}$$

with the following boundary conditions,

$$\frac{\partial p_r}{\partial x} - \rho g = 0 \quad \text{at} \quad x = L, \tag{12}$$

$$p_r = P \quad \text{at} \quad x = 0, \tag{13}$$

where k_z is the root axial hydraulic conductivity calculated using Poiseuille's law ($m^4\ Pa^{-1}s^{-1}$), P is the initial water pressure (Pa) and L denotes the maximum length of the root system (m). The single root uptake equation is scaled up using the multi-scale analysis presented in Roose and Fowler (2004) to represent macroscopic behaviour (e.g. many roots within a vegetated soil profile) in determining F_W with the depth of the soil.

The model is written in terms of relative water saturation (S) as it is more stable to numerically solve for Richards equation via a finite volume method. To summarise, the one dimensional model describing water movement in the soil and plant water uptake is,

$$\frac{\partial S}{\partial t} = \frac{\boldsymbol{\partial}}{\boldsymbol{\partial z}}\left[D_0 D(S)\frac{\boldsymbol{\partial S}}{\boldsymbol{\partial z}} - K_s K(S)\right] - F_W \tag{14}$$

where

$$F_W = 2\pi a l_d k_r(-p_c f(S) - p_r). \tag{15}$$

The boundary conditions for the model are

$$D_0 D(S)\frac{\partial S}{\partial x} - K_s K(S) = \begin{cases} -W & at \quad x=0, \\ 0 & at \quad x=l_w. \end{cases} \tag{16}$$

The root internal pressure p_r is calculated from

$$2\pi a k_r(-p_c f(S) - p_r) = -k_z \frac{\partial^2 p_r}{\partial x^2}, \tag{17}$$

with

$$\frac{\partial p_r}{\partial x} - \rho g = 0 \quad \text{at} \quad x = L, \tag{18}$$

$$p_r = P \quad \text{at} \quad x = 0. \tag{19}$$

The following sections validate this model against the soil saturation data provided by Smethurst et al (2012).

3.2. Adjustments to the model and dataset

Figure 3a shows the water content measured with the TDR probes at different depths at location A for the year 2005. A reduction in the water content is observed at 0.3 m, 0.45 m and 0.6 m depths between June and October, reflecting the summer drying period. The traces for the shallowest three probes show a series of short upward spikes in response to heavy winter rainfall events. The spikes in water content are likely caused by pulses of water passing downward through the upper (more silty) part of the profile after heavy rainfall events, returning after the event to field capacity (the equilibrium water content of soil held against gravity).

The very rapid spikes in the measured traces of water content were difficult to model as they were misleading the model fitting procedure. The model cannot represent these short time dynamic conditions, as it is designed to track seasonal variations on the timescale relevant to plant water uptake rates than response to fast hourly/daily extreme weather events. It was decided therefore to focus on modelling the saturation level at field capacity during the winter, and its reduction during the summer and early autumn. A Fourier Transformation Signalling algorithm (Smith 1997) was used to eliminate the spikes found in raw data and produce smoother curves that reflect the long-term change in the soil saturation level. The algorithm uses the following equation:

$$p(x) = \sum_{k=0}^{N} a_k \cos(kx) + b_k \sin(kx), \tag{20}$$

where a_k and b_k are variables to be solved for a fixed N and at a set of chosen points, x, and their value $p(x)$. The spike smoothing process involves taking uniformly spaced points along the x-axis and smoothing the curve between them using equation (20). The result of this process is shown in Figure 3b which shows the smoothed data for the corresponding raw data in Figure 3a. Initially curves consist of about 2000 data points, which when smoothed reduce to about 50 data points. In order to generate a full data set again, the 50 data points are extrapolated back to 2000. The sum of squares scores between the original and new (with spikes removed) data sets is low at an average of 2.7 for location A and 0.2 for location C. The smoothing method eliminates the peaks while maintaining the main characteristics of the curves and from now on mention to the probe/experimental data is referring to the smoothed data, of Figure 3b.

The water flux at the ground surface is modelled by considering the net flux of water into the soil W, which is based on environmental factors such as rainfall (R), humidity (H), wind speed (WS), temperature (T) and a constant (c), using either linear (equation 21) or non-linear (equation 22) expressions,

$$W = \delta R + \alpha H + \beta T + \gamma WS + c\,, \tag{21}$$

$$W = \delta R + \alpha_1 H + \alpha_2 H^2 + \alpha_3 H^3 + \beta_1 T + \beta_2 T^2 + \beta_3 T^3 + \gamma_1 WS + \gamma_2 WS^2 + \gamma_3 WS^3 + c\,, \tag{22}$$

where the parameter vectors $\delta, \alpha, \beta, \gamma$ and c are to be determined from the optimal fit to the soil water content data of Smethurst et al (2012). The flux of water W has units $ms^{-1}$of water and from this units can be assigned to the remaining parameters as shown in Table 1. Equations (21) and (22) can essentially be considered as Taylor expanded versions of other non-linear relationships often used for calculation of evaporation/transpiration such as the Penman-Monteith equation.

The driving pressure (P) inside the root is dominated by atmospheric humidity and temperature as the stomata in the leaves open and close depending on the environmental conditions (Tuzet et al,

2003). When the air temperature is high and/or humidity is low the plant closes its stomata to slow down the loss of water and this leads to an increase in the pressure of water inside the roots. Due to the direct change to the water pressure within the plant roots, we use the following formula for P for the boundary equation (19) to model the total pressure,

$$P = (p_r^0 + \lambda_3) + \lambda_1 T + \lambda_2 H, \tag{23}$$

where p_r^0 is the baseline root pressure and $\lambda_1(\mathrm{Pa/degC})$, $\lambda_2(\mathrm{Pa/\%\ humidity})$ and $\lambda_3(\mathrm{Pa})$ are determined by seeking the optimal fit to the soil water content data. The parameter values are given in Table 1 while the inputs and outputs for this model are given in Table 2.

4. Methods

4.1. Numerics

To solve equations (14)--(19) numerically the x-axis was discretised into 800 equidistant points over the depth of the assumed soil profile (0 to 2 meters depth). A high-resolution Monotone Upstream-centred Schemes for Conservation Laws (MUSCL) proposed by Kurganov and Tadmor (2000) was used which set 1600 cells as that required to obtain the true solution for the soil profile; it was found that 800 cells gave a less than 1% error for the model output (plant water uptake) with a significant reduction in run time (between a factor of 5 and 6) and this was selected as the final grid size.

4.2. Validation techniques

In Roose and Fowler (2004) the flux of water into the soil at the soil surface (W) and the pressure inside the root (p_r) were set to have a constant value in time. To more accurately represent the effect of the climate on these factors they were set as external time dependant inputs.

Equations (21) and (22) for the flux of water into the soil (W, in essence rainfall minus the runoff and evaporation) are simpler than other models for potential evapotranspiration (PET) such as the

Penman-Monteith equation (Allen et al, 1998). Simple linear and non-linear relationships between evaporation/ evapotranspiration, temperature, humidity and wind speed (similar to equations 21 and 22) have been proposed in the literature, and demonstrated to work well for site specific locations (Fisher et al, 2005; Bormann, 2011).

The water flux into the soil is calculated from the climate data collected by Smethurst et al (2012). Since the characteristics of the climate data vary across the different seasons, the climate data were split into blocks of about 3 months representing each of winter, spring, summer and autumn, and the model used to simulate each 3 month period separately. The initial model starting condition for each seasonal period was based on the finishing point of the preceding season.

The field data are taken from a highway cutting in which the ground slopes at about 16 degrees. Briggs et al (2013) carried out both a one- and two-dimensional unsaturated finite element simulation of a clay slope, with the one-dimensional column model having the same vertical geometry as the mid-slope of the two-dimensional model. Both were analysed with the same surface boundary flux representing climate and vegetation, and the results of the one-dimensional column model agreed closely with the two-dimensional model. This was because horizontal water flow due to gravity was found to be small compared with vertical water flow due to the flux boundary at the ground surface. It was therefore considered reasonable to model the effects of the vegetation here in one-dimension only. In this case, use of a one-dimensional model allows an optimisation of some of the soil parameters (described in section 4.3) that would be difficult to do with a two-dimensional model. The impermeable base of the model was assumed to be at 2 m depth. This was based on there being only a small change in measured water content and pore pressure at this depth (Smethurst et al, 2012) with most of the change due to the vegetation occurring in the top 0.8 m of the profile. The impact of a more diffuse boundary condition at the bottom could be investigated within future work.

The water permeability in fully saturated soil k_s and the soil suction parameter m are linked in equation (7), and control how the water moves through an unsaturated soil. These values were assumed to be constant in the original model by Roose and Fowler (2004). However, measurements and modelling indicate that these values can vary both with depth and time (e.g. Anderson et al 1982; Li et al 2011). For example, surface soils are often quite structured with a higher organic matter content and larger cracks/fissures caused by root penetration and repeated drying and wetting cycles. A greater number of larger voids in the soil will give a lower air entry value and more rapid water drainage from the soil at lower suction, thus changing the shape of the soil water retention curve (SWRC). In this case, there are no site specific data for variation of m with depth, and few if any measurements of this type appear to have been carried out for a stiff clay soil. The parameter m was allowed to vary to obtain an optimal fit to the water content data, with m modelled using a bounded arbitrary function. The value of m was allowed to change between the points at which the experimental water content levels were recorded (at 0, 0.3, 0.45, 0.6, 0.9 and 1.5m), giving 6 different values of m for the full soil profile. The values of m were optimised for each of seasonal time periods considered.

At location A there is a variation of soil characteristics with depth, going from a layer of more silty weathered London Clay at the top to a layer of lower permeability grey London Clay below (Fig. 1). This transition occurs around x_2=0.9m, which for the purpose of the numerical simulations is taken to be an exact depth (Fig. 4). Two scenarios were considered for location A: in scenario 1 (Fig. 4a), k_s has a constant value for both types of soil, whereas in scenario 2 (Fig. 4b), k_s linearly decreases with depth in the weathered London Clay region and is constant in the grey London Clay. Since location C consists only of grey London Clay, k_s was set to linearly decrease with depth, as seen in scenario 3 (Fig. 4c). Some measured data for permeability at the site were available, from deeper depths in the clay (mainly below 1.0 m; Smethurst et al, 2012). The site data were used to define the value of k_s at depth, and arbitrary increases were applied to the relevant scenarios above this. The model is found to be more sensitive to changes in m compared to k_s, hence the values of k_s were held constant

over the full year of modelled data where scenario 2 was set for location A, and scenario 3 was set for location C. This means that the model does not incorporate the influence of potential surface desiccation cracking. Evidence is investigated in Section 5 to support the hypothesis that water permeability decreases with greater depths.

The exact root distribution of the vegetation at the site in Newbury is not known and the water uptake parameter k_r and root length density l_d were set as constant with time within each seasonal period but allowed to vary between these. It was assumed the roots at the Newbury site had already grown to full length, and the length of the main root (zero order) was fixed at $0.8\ m$.

4.3 Optimisation Procedure

The model output is the optimal set of values for the following parameters: 2 for the water uptake (equation 17), 2 for the root length parameters (equation 15), 5 or 11 respectively for the linear or non-linear systems for the flux of water at the soil surface (equations 21 and 22), 3 for the water pressure inside the root (equation 23) and 6 for the Van Genuchten soil suction parameter m. This set of parameters was combined with the model to produce an accurate representation of the water movement within the soil, from the given climate data and the root and soil parameters seen in Table 1.

An upper bound for the input flux of water W was imposed, because at high values of rainfall (conditional to parameters such as water uptake into the plant roots and water diffusivity) the model becomes invalid as the soil profile becomes fully saturated, and equation (16) no longer holds. The upper bound was distributed between the parameters in equations (21) and (22), as they sum to the value of W. These bounds restricted the parameters to be within realistic values and Table 1 shows the enforced upper bounds. The experimental data show that the surface was never fully saturated and therefore equation (16) holds for unsaturated soil.

Once the values for the flux of water W are determined together with the rest of the model parameters, equation (14) can be solved numerically to obtain the resulting water profile. The calculated water profile was then compared to the experimental data (i.e. the values for the water content at different depths) by using the sum of squares differences between observed and simulated data. Equation (24) denotes the formula for the sum of squares (SOS) difference for the objective value y

$$y = \sum_{i=1}^{N}(x_i - \bar{x}_i)^2, \tag{24}$$

where x_i are the model points and $\bar{x}_i$ are the data points, for a set of N points. The optimisation procedure used the global optimisation method Kriging, from Forrester et al (2008), which stops as the objective value either reaches 0, shows no sign of change after a set number of iterations, or until a maximum number of iterations has occurred. A large number of the simulation runs stopped due to no sign of change as they converged on the global/local optima.

As described above, the simulation has up to 24 parameters in the non-linear case and just one output, the sum of squares fit. An optimisation procedure was used as opposed to an exhaustive search (evaluating every combination), to find the optimal set of parameters which minimises the sum of squares fit. The optimisation procedure was twofold; firstly a set of initial starting points are chosen and then evaluated; secondly a process takes these points and converges on an optimal solution.

The initial search plan was based on the Latin Hyper Cube Technique (Iman et al, 1980), where the points picked are as far away from each other as possible. This method uses a Genetic Algorithm to optimise for the greatest distance between the initial points. The conventional number of points to pick is 10 times the number of dimensions (parameters).

Once these initial search points are found their objective value was calculated using the full model given in section 3. The next set of points to be sampled was calculated from the Kriging algorithm (Forrester et al, 2008), which produced a surrogate model to imitate the full model. The Kriging procedure was iterative and used all of the information from the points calculated at the previous time step to estimate the best local and global points using two techniques; exploitation and exploration. Exploitation works like a local search or hill climber, as opposed to exploration which fills the gaps between existing sample points, placed at the maximum estimated error. These points were found on the surrogate model as it was much less expensive to traverse and find potentially optimal points within the surrogate than for the full model. This process was continued until the desired stopping condition was reached, which depended on the convergence of the optimal set of parameters, the number of sample points and the value of the expected improvement.

5. Results

The model was validated using the climate data from Smethurst et al (2012) following the approach described in section 4. The difference between the sum of squares fit for the two locations A and C, with linear and non-linear expressions for the climate input data, and the different seasons (wet and dry periods), is compared below. The profile of the Van Genuchten parameter *m* is also considered.

5.1 Fitting the 2005 data

Figure 5 shows the fitting for the whole year (reconstructed from the seasonal segments) for all of the probes in both locations A and C for the year 2005 for a linear formulation of the climate conditions, and demonstrates that the model simulation accurately represents the soil water content. The model fluctuates a little around the experimental data, and better fits were obtained at deeper depths due to the smaller overall change in the water content.

In Figure 5 there are large differences between the model and experimental data in the autumn season, indicating a poor fit, especially for 0.6 m depth at location A. This is in contrast to the other seasons where good fits are obtained. The reason for the poor fit in autumn is due to the change in climate and soil conditions from mid-October to mid-November, where there is a large and sudden increase in the soil water content at 0.3m depth from 0.17 to 0.36. In this period the model changes more slowly than the measured trace, and takes several days to catch up with it, matching it again in December when the winter season starts. This could be due to the saturated values for permeability used in the model, which may not reflect the near-surface clay cracking that occurs during the summer period. The model does not capture the hysteresis of the SWRC, which would also potentially allow a rapid increase in water content on wetting.

Better fits were obtained for the sum of squares (SOS) values for location C compared to location A by roughly a factor of 2.5, when normalised. The fittings are much tighter for location C than location A, especially at 1.5 m depth. However, in autumn at 0.3 m depth the fitting again takes some time to catch up with the sudden increase in measured water content. In winter and spring, the model fits the data very well, especially at location C where the SOS values are below or close to 1. The smoothed experimental data for location A provided a better landscape for the model fit compared to the raw data.

There was found to be little difference in the model fit to the field data resulting from the linear and non-linear climate expressions, equations (21) and (22) respectively. However, there was a difference between the different locations and seasons as seen in Table 3, which shows the final sum of squares scores for each of the scenarios.

5.2 Soil suction parameter (m)

The Van Genuchten soil suction parameter m denotes a fitting parameter which is normally determined by fitting a curve to data points obtained experimentally from samples of soil. Small

samples of soil are usually tested under zero total stress, and the laboratory results may not capture either the bulk structure of the soil (and its variability throughout locations A and C), nor the likely change in water retention properties with increasing total stress. It would not be unreasonable to expect the value of m to change, both between locations A and C, and with depth below the ground. The effects of volume changes and stress states have been considered on the SWRC by Ng and Pang (2000), who show that under higher stress there are lower rates of desorption, likely caused by the existence of average smaller pore size distributions in the soil. The value of p_c which largely controls the air entry value of the SWRC was fixed at a value of 23 kPa, intended to be representative of a structured clay soil (Briggs et al, 2013). Changes in the air entry value due to the particle size and structure of the soil, and changes in soil stress, are thus not modelled; this is a limitation of the current simulations and may be incorporated in further investigations.

In analysis of the SWRC, an increase in the value of m gives a smaller value of soil suction for the same value of volumetric water content; thus coarser soils or those with structure should have water retention behaviour defined by higher values of m. At higher stresses the pore sizes will decrease, consistent with a smaller value of m at depth.

Previous models (ROSETTA by Schaap et al, 2001 and a plant water uptake model by Roose and Fowler, 2004) use one value of m for the full soil profile, but here the optimisation was able to determine the values for m that produce the best fit to the measured water content data. The results of the optimisation procedure showed that the profile of m with depth generally conformed into one distribution, where the averages are seen in Figure 6.

The profiles in Figure 6 indicate that the value of m varies with depth. The four profiles for locations C and A (linear and non-linear formulation of the climate conditions) are very similar. Below 0.9m the value of m is fairly uniform with depth, perhaps as a result of increasing soil uniformity deeper within the profile. For the layer of soil between 0 and 0.9m there is an increase in the value of m immediately below the soil surface followed by a decrease. A high value of m indicates a coarser soil,

which is consistent with a generally more structured soil around the root system. As explained earlier, water permeability changes with depth (Li et al, 2011) and it is therefore plausible that m will also change with depth (they are coupled by equation 7). Ghanbarian-Alavijeh et al, (2010) estimated values for m using a fractal approach, for different soil types, and improved the root mean square error values given from the ROSETTA model. However, the range of values estimated for m still differed widely; for example in a silty clay loam the maximum and minimum values were 0.48 and 0.09 respectively. No experimental studies seem to have been carried out to quantify the change in m with depth within a stiff clay; nonetheless the profiles obtained from the model look sensible, and in future could be checked against experimental measurements.

5.3 Predictions and comparisons

To test how effective the validation of the model was, the optimal fitting parameters from the 2005 validation were used to run the model for the following year, 2006. Figure 7 shows the results of the model plotted with the experimental data for 2006; these look quite similar to that of 2005 (Fig. 5), where the model achieved a good fit. The SOS scores for the 2006 model run (Table 3) are slightly worse than for the 2005 fitting procedure as may be expected; the 2006 scores were approximately twice as large, summing over the year. Averaging the input parameters from 2 or more years of fittings would help improve the forecasting ability, as the unknown soil and water parameters would likely be matched to a higher degree of accuracy with more available data.

The average soil water content from the model was compared with that calculated using CROPWAT with the Penman-Monteith equation, as used by Smethurst et al (2012) to model the same site. Figure 8 shows the comparison of the CROPWAT model, the updated Roose and Fowler model, and the average soil water content for locations A and C calculated from the TDR probe data (a weighted average of the probe readings at different depths). Throughout the year the average water content at location C is 11% lower than location A, despite the climate conditions being equal. This is due to the different soil properties between the measurement locations, and the different initial saturation

of the soil. The updated Roose and Fowler model accounts for this whereas the simple water balance in CROPWAT does not. The Roose and Fowler model produces a much better fit to the TDR probe data, due to the more detailed mathematical formulation used to describe the plant, soil and water movement, when compared with models such as CROPWAT which produce an average value for the depth of the soil column.

A separate sensitivity analysis on all of the parameters in the model was carried out; where the new SOS score was calculated after individually changing each parameter by ±5%. It was found that the most sensitive parameters were those associated with the pressure in the xylem vessels, i.e. plant parameters appear to be very important. This indicates that it is important that the good estimates of these parameters are determined (if they can be experientially measured, which is the case) and future work will involve more careful measurements and modelling of the pressure in the xylem vessel.

Finally, to demonstrate that the parameter optimisation procedure is valuable when dealing with large parameter uncertainty, the model was used to fit the 2005 data, but this time using fixed and uniform with depth 'best guess' values for k_s and m. This model run (Fig. 9) gave poor results with an SOS of 203. The fittings at 0.45 and 0.6m were acceptable due to the value of m being close to the earlier values used at these depths. However, the model did not match the other probe depths well, as there was a difference in the value of m from the fully optimised model fit. This also supports the idea that k_s and m are depth dependent, and that outputs from models of this type can be sensitive to having the correct soil-water parameters.

6. Discussion

The modified Roose and Fowler (2004) model has made use of climate data and soil information to estimate the water content within the soil. It provides a variation in water content with depth in the soil profile rather than an average such as obtained from simple water balance models. The

proposed model also estimates the uptake of water into plant roots. A procedure for fitting the model to measured data has been used to estimate and optimise soil-water and plant parameters which may be particularly uncertain and to which the outputs from this type of model can be particularly sensitive.

The fitting procedure was used on water content data measured at a clay cutting slope site near Newbury, Berkshire. The changes made to the profiles for saturated water permeability k_s (Figure 4) had relatively little effect on the model outputs compared to the change in the Van Genuchten soil suction parameter m. The permeability does vary with saturation (equation 4), however, permeability was not allowed to sufficiently increase to represent clay cracking, and this resulted in generally poor model fits to the real data during the autumn/winter soil re-wetting. The model could be adjusted to allow optimisation of saturated permeability, as well as the water retention parameter m. The profiles of m from the model output (Fig. 6) show an average larger pore size for the root zone; this is where the soil is likely to be more disturbed or structured in practice.

A sensitivity analysis was carried out and showed that the most sensitive parameters in the model were those involved with the pressure in the xylem vessel. It is therefore important to measure these plant parameters accurately; to help with this, the optimisation procedure is useful for estimating values that are uncertain.

The model may be used for sites such as vegetated clay earthworks to estimate the extent of drying and effective stress changes in the soil in response to climate or changes in vegetation. Where measured water content or pore water pressure data are available, these may be used with the fitting procedure to assess difficult parameters such as k_s and m.

The model has the potential to be used for different soil types, climate conditions and for growing root systems; as long as the set of parameters in Table 1 are obtained or estimated. Therefore the

model should aid soil and plant management strategies through better understanding the soil and water configuration, and by forecasting soil conditions for potential scenarios.

Acknowledgements

We would like to thank the EPSRC for funding J. Smethurst (grant numbers GR/R72341/01 and EP/F063482/01), the BBSRC for funding S. Payvandi, The Royal Society University Research Fellowship for funding T. Roose, Award No. KUK-C1-013-04 of the king Abdullah University of Science and Technology (KAUST) for funding K. Zygalakis, EPSRC and CORMSIS for funding J. Fliege and EPSRC Complexity DTC for funding J. Heppell (EP/G03690X/1). The Authors acknowledge the use of the IRIDIS High Performance Computing Facility, and associated support services at the University of Southampton, in the completion of this work.

References

Allen, R. K., Smith, M., Perrier, A. & Pereira, L. S. (1994). An update for the calculation of reference evapotranspiration. ICID Bull. 43, No. 2, 35–92.

Anderson, M. G., Hubbard, M. G. Kneale, P. E. (1982). The influence of shrinkage cracks on pore water pressures within a clay embankment. Quarterly Journal of Engineering Geology and Hydrogeology. 15(1): 9-14.

Andrei, A. (2000). Embankment stabilisation works between Rayners Lane and South Harrow Underground stations. Ground Engng, 33, No. 1, 24-26.

Benton, T., Gallani, B., Jones, C., Lewis, K., Tiffin, R. & Donohoe, T. (2012). Severe weather and UK food chain resilience – Detailed Appendix to Synthesis report. Global food security. http://www.bis.gov.uk/go-science.

Bormann, H. (2011). Sensitivity analysis of 18 different potential evapotranspiration models to observe climatic change at German climate stations. Climatic Change 104:729-753. DOI 10.1007/s10584-010-9869-7.

Briggs, K. M., Smethurst, J. A., Powrie, W. & O'Brien, A. S. (2013). Wet winter pore pressures in railway embankments. Proceedings of the Institution of Civil Engineers - Geotechnical Engineering 166, (GE5), 451-465. (doi:10.1680/geng.11.00106).

Clarke, D., Smith, M. & El-Askari, K. (1998). CropWat for Windows: User guide, Version 4.2, www.fao.org.

Clarke, D., Smith, M. & El-Askari, K. (1998). New software for crop water requirements and irrigation scheduling. ICID Bull. 47, No 2, 45–58.

Clarke, D. & Smethurst, J. (2010). Effect of climate change on cycles of wetting and drying in engineered clay slopes in England. Quarterly Journal of Engineering Geology and Hydrogeology, **43**: 473-486.

Croney, D. (1977). Design and Performance of Road Pavements. Her Majesty's Stationery Office, London, UK.

Driscoll, R. 1983. The influence of vegetation on the swelling and shrinking of clay soils in Britain. Géotechnique, 33, 93–105.

Fisher, J., DeBiase, T., Qi, Y., Xu, M. & Goldstein, A. (2005). Evapotranspiration models compared on a Sierra Nevada forest ecosystem. Environmental Modelling & Software. 20, No.6, 783-796.

Forrester, A., S*ó*bester, A. and Keane, A. (2008). Engineering Design via Surrogate Modelling: A practical Guide. John Wiley & Sons.

Ghanbarian-Alavijeh, B., Liaghat, A., Guan-Hua, H. and Van Genuchten, M. (2010). Estimation of the van Genuchten soil water retention properties from soil textural data. Pedosphere 20, No.4, 456-465.

Iman, R. L., Davenport, J. M., and Zeigler, D. K. (1980). Latin Hypercube Sampling (A Program User's Guide). Tech. Report SAND79-1473, Sandia National Laboratories, Albuquerque, NM.

Jones, J., Hoogenboom, G., Porter, C., Boote, K., Batchelor, W., Hunt, L., Wilkens, P., Singh, U., Gijsman, A. and Ritchie, J. (2003) The DASSAT cropping system model. European Journal of Agronomy, 18, 235-265.

Jury, A. & Vaux, H. (2005). The role of science in solving the world's emerging water problems. PNAS. 102, No 44, 15715-15720.

Kurganov, A. and Tadmor, E. (2000). New high-resolution central schemes for non-linear conservation laws and convection-diffusion equations. Journal of Computational Physics. 160, No.1, 241-282.

Li L. J. H., Zhang, L., Kwong B. C. P. (2011). Field permeability at shallow depth in a compacted fill. Proceedings of the Institution of Civil Engineers: Geotechnical Engineering. 164 (3): 211-221.

Loveridge, F. A., Spink, T. W., O'Brien, A. S., Briggs, K. M. & Butcher, D. (2010). The impact of climate and climate change on UK infrastructure slopes. Q. J. Engng Geol. Hydrogeol. 43, No. 4, 461–472.

McCown, R., Hammer, G., Hargreaves, J., Holzworth, D. and Freebairn, D. (1996) APSIM: a novel software system for model development, model testing and simulation in agricultural systems research. Agricultural Systems. 50, 255-271.

Ng, C. and Pang, Y. (2000). Experimental investigations of the soil-water characteristics of a volcanic soil. Canadian Geotechnical Journal. 37, No. 6, 1252-1264.

Nyambayo, V. and Potts, D. (2010). Numerical simulation of evapotranspiration using a root water uptake model. Computers and Geotechnics. 37, 175-186.

O'Brien, A. (2007). Rehabilitation of urban railway embankments: investigation, analysis and stabilisation. In Proceedings of the 14th European Conference on Soil Mechanics and Geotechnical Engineering, Madrid (Cuellar V, Dapena E, Alonso E et al. (eds)). Millpress, Amsterdam, the Netherlands, pp. 125-143.

Pimentel, D., Berger, B., Filiberto, D., Newton, M., Wolfe, B., Karabinakis, E., Clark, S., Poon, E., Abbett, E., and Nandagopal, S. (2004). Water Resources: Agricultural and Environmental Issues. BioScience. 54, No. 10, 909-918.

Rahardjo, H., Li, X., Toll D. and Leong, E. (2001). The effect of antecedent rainfall on slope stability. Geotechnical and Geological Engineering. 19, 371-399.

Roose, T. and Fowler, A. (2004) A model for water uptake by plant roots. Journal of Theoretical Biology, 288, 155-171.

Rouainia, M., Davies, O., O'Brien, A. & Glendinning, S. (2009). Numerical modelling of climate effects on slope stability. Proc. Instn Civ. Engrs Engng Sustainability 162, No. ES2, 81–89.

Schaap, M., Leij, F. and Van Genuchten, M. (2001). ROSETTA: a computer program for estimating soil hydraulic parameters with hierarchical pedotransfer functions. *Journal of Hydrology* 251, 163-176.

Smethurst, J. A., Clarke, D. & Powrie, W. (2006). Seasonal changes in pore water pressure in a grass covered cut slope in London Clay. Geotechnique 56, No. 8, 523–537.

Smethurst, J., Clarke, D. and Powrie, W. (2012) Factors controlling the seasonal variation in soil water content and pore water pressures within a lightly vegetated clay slope. Geotechnique, 62, (5), 429-446.

Smith, S. (1997) The scientist and Engineer's Guide to Digital Signal Processing. California Technical Publishing San Diedo, CA, USE. ISBN: 0-9660176-3-3.

Tuzet, A., Perrier, A. and Leuning, R. (2003). A coupled model of stomatal conductance, photosynthesis and transpiration. Plant, Cell & Environment. 26, No. 7, 1097-1116.

Van Genuchten, M. (1980) A closed-form equation for predicting the hydraulic conductivity of unsaturated soil. Soil Sci. Soc Am. J., 44, 892-898.

Vaughan, P.R., Kovacevic, N. & Potts, D.M. (2004). Then and now: some comments on the design and analysis of slopes and embankments. In: Jardine, R.J., Potts, D.M. &Higgins, K.G. (eds) Advances in Geotechnical Engineering: Proceedings of the Skempton Conference, Imperial College, London, 1. Thomas Telford, London, 241–290.

List of Figures

List of Tables

Figures

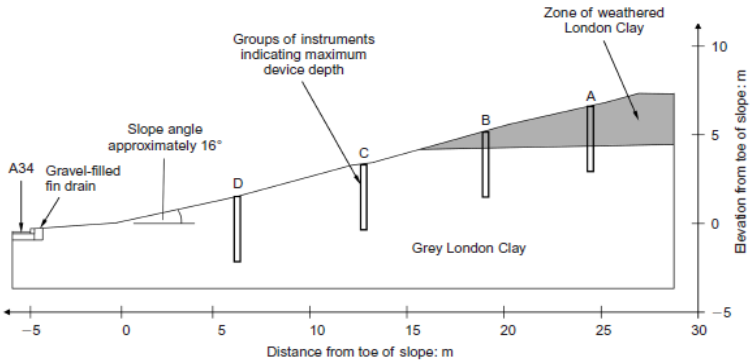

Figure 1: A cross section through the Newbury site showing the locations of installed instrumentation. Taken from Smethurst et al (2012).

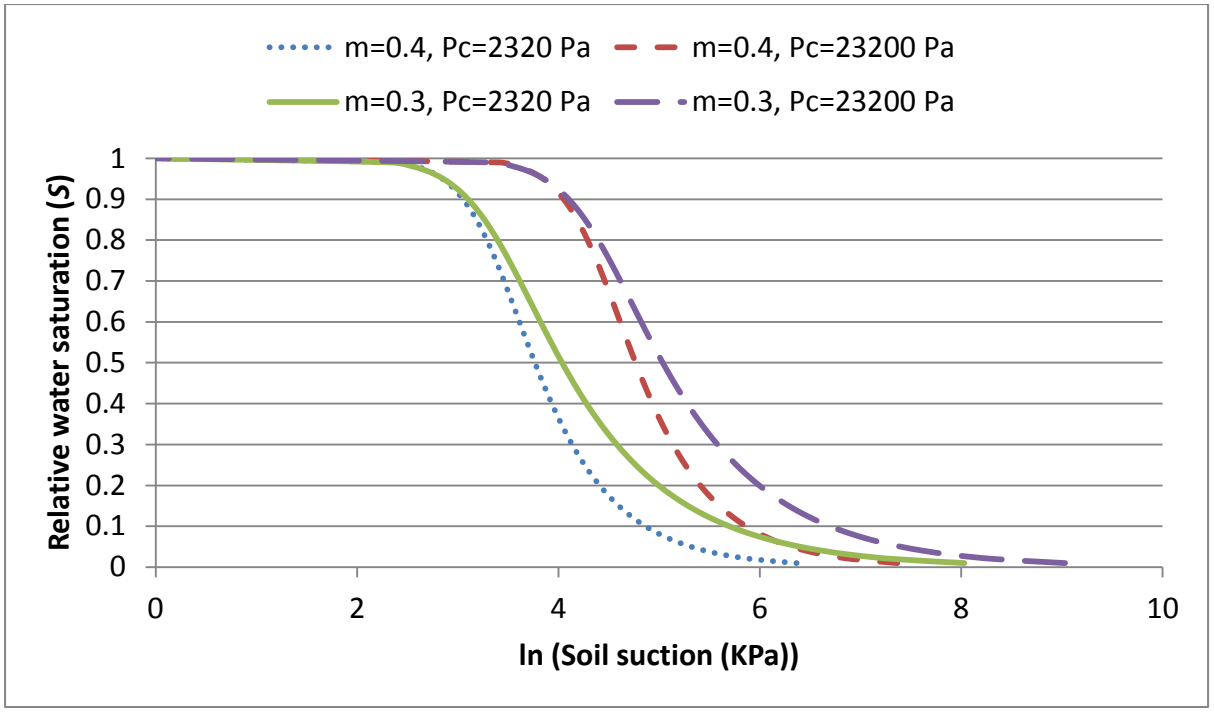

Figure 2: Soil water retention curves for two different values of m (0.3 and 0.4) and p_c (23200 Pa and 2320 Pa). The curves for p_c = 23000 Pa are representative of those used to model the Newbury site.

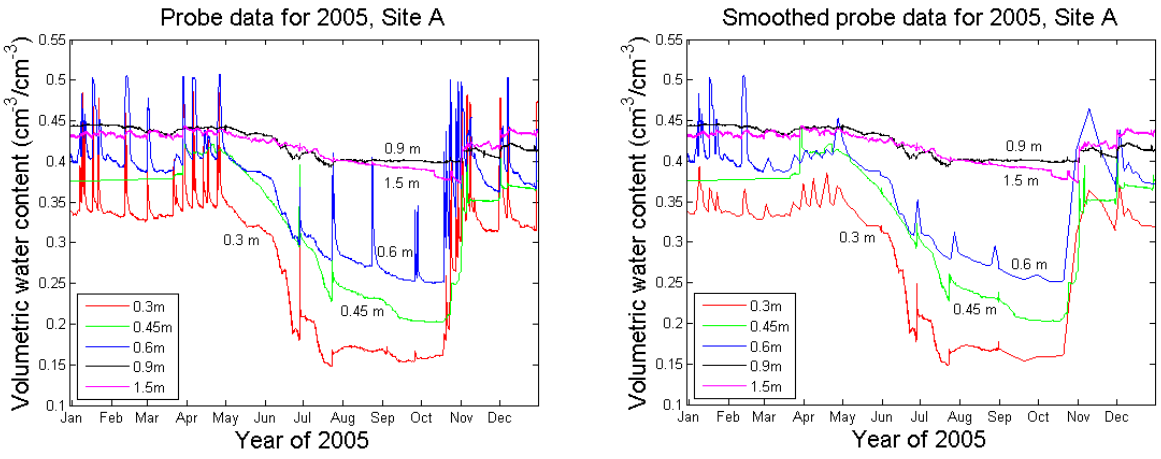

(a) (b)

Figure 3: TDR probe data at location A for 2005 showing the volumetric water content at different soil depths: (a) the raw data; and (b) the data smoothed by the Fourier Transformation signalling algorithm.

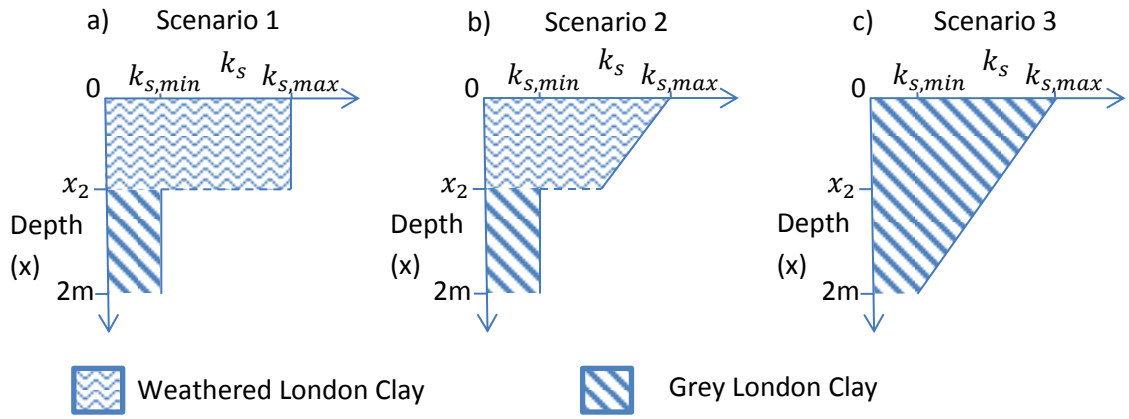

Figure 4: Three scenarios used to model the change in saturated water permeability (k_s) with depth.

The value of k_s is bounded between $k_{s,min}$ and $k_{s,max}$ which are 5.78x10^{-9} and 5.78x10^{-8} m^2 respectively (Table 1).

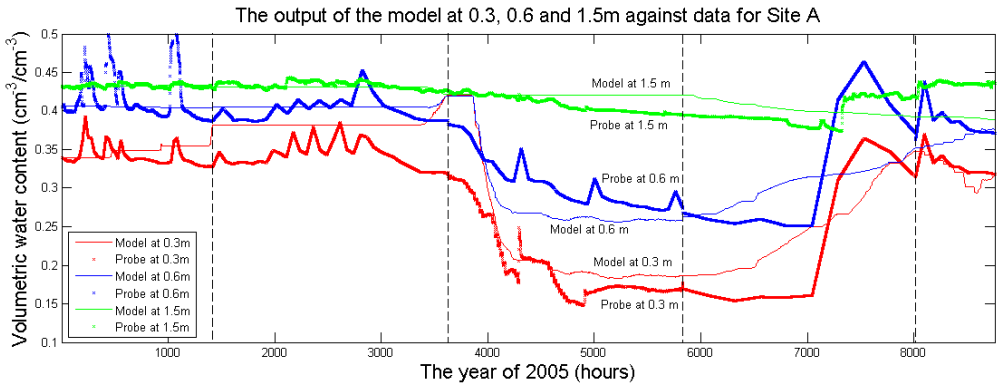

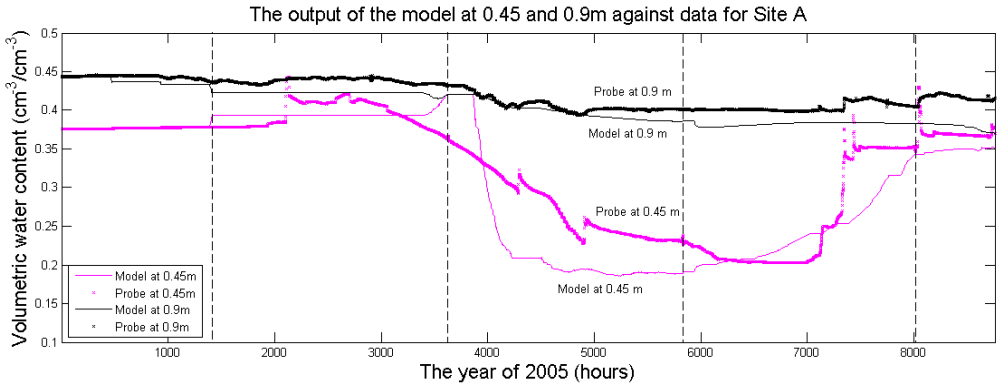

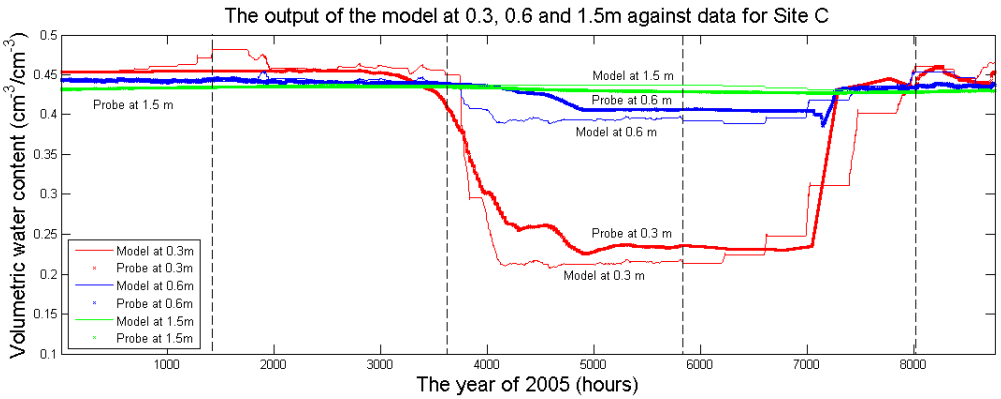

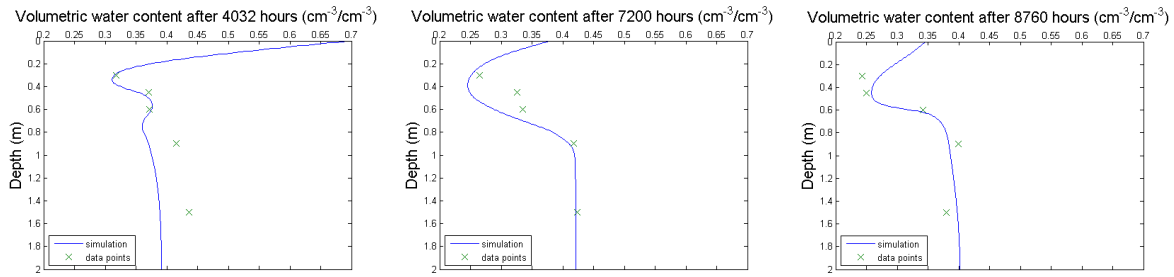

Figure 5: The model fittings for 2005 for locations A and C for five and three probe depths, respectively, with a linear formulation of the climate conditions. The bottom three snapshots are taken at 4032, 7200 and 8760 hours respectively.

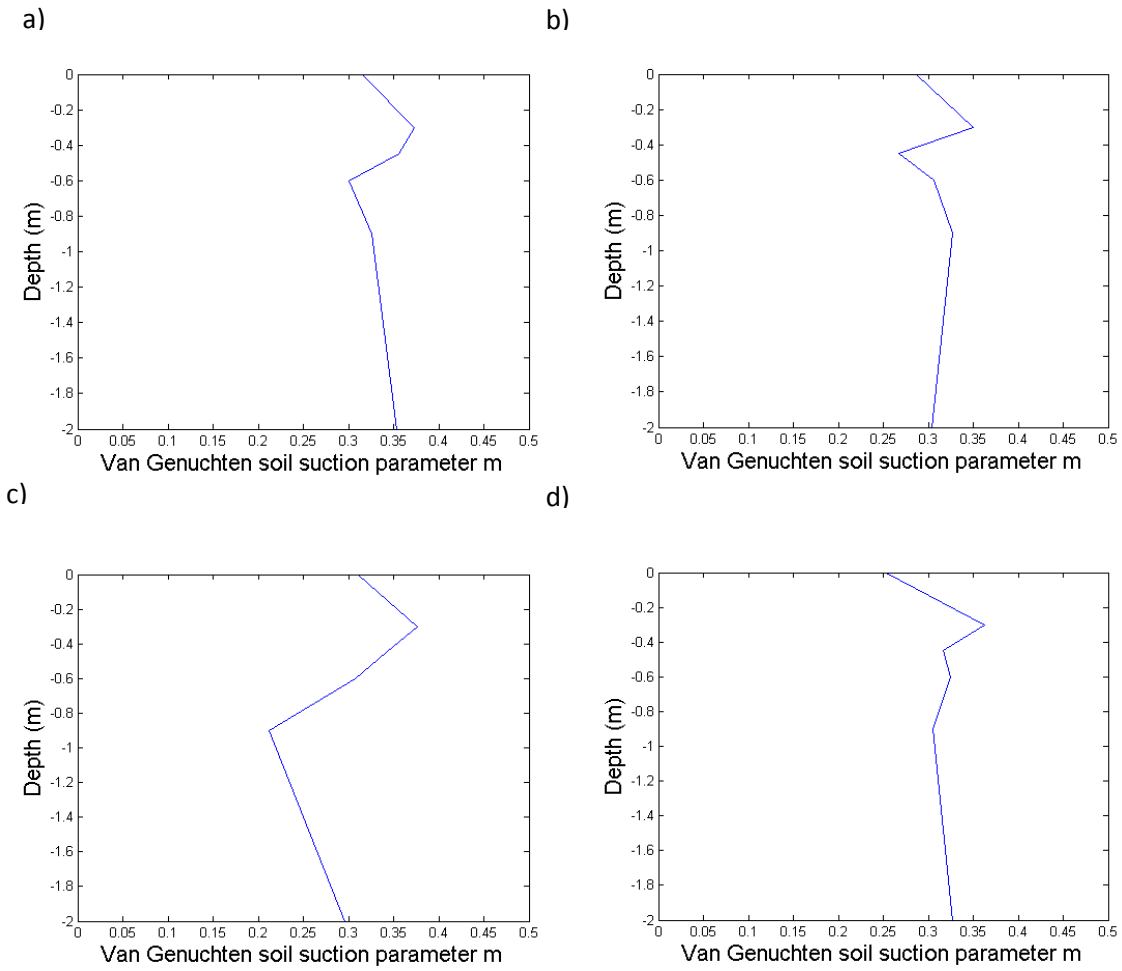

Figure 6: The averaged seasonal profile for m for locations A (a, c) and C (b, d) with linear and non-linear input water flux formulations respectively.

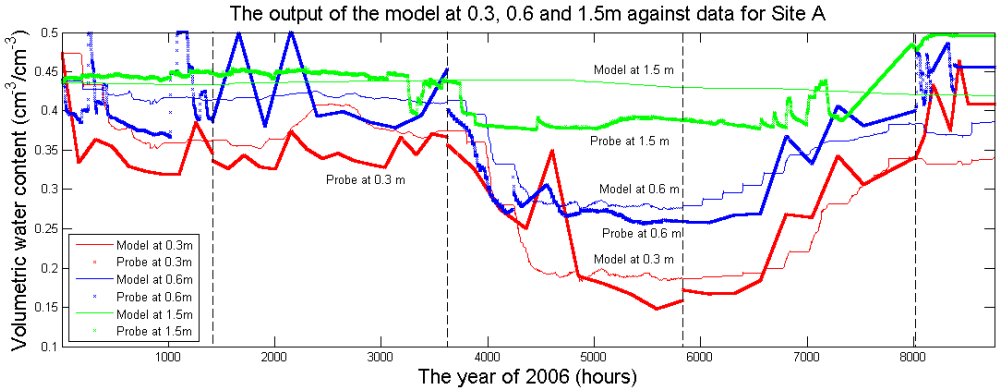

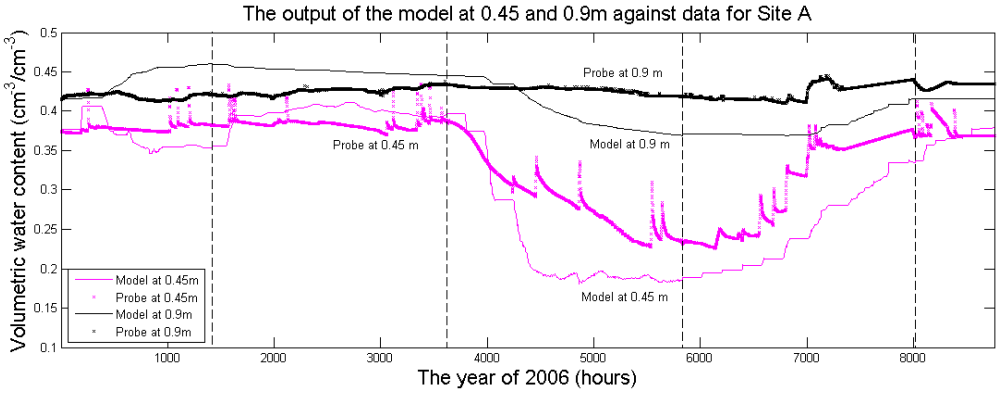

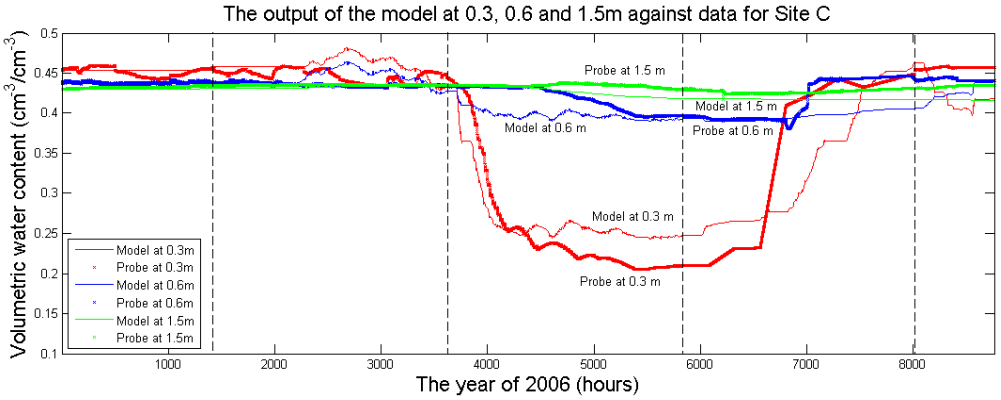

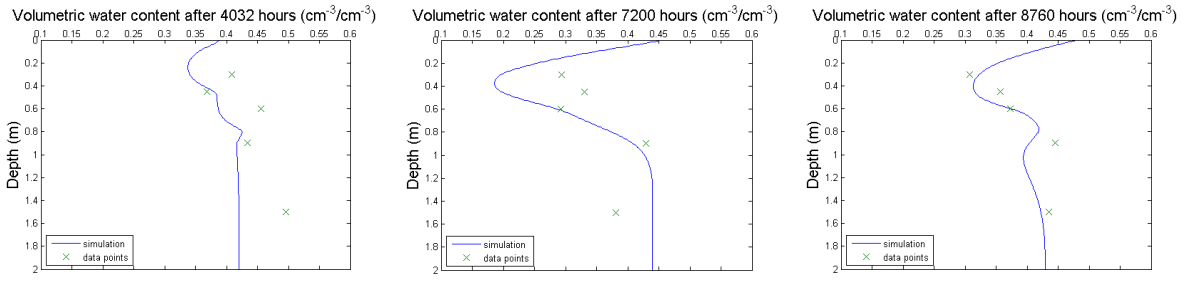

Figure 7: Model run to forecast water content changes in 2006 for locations A and C for five and three probe depths, respectively, with a linear formulation of the climate conditions. The bottom three snapshots are taken at 4032, 7200 and 8760 hours respectively.

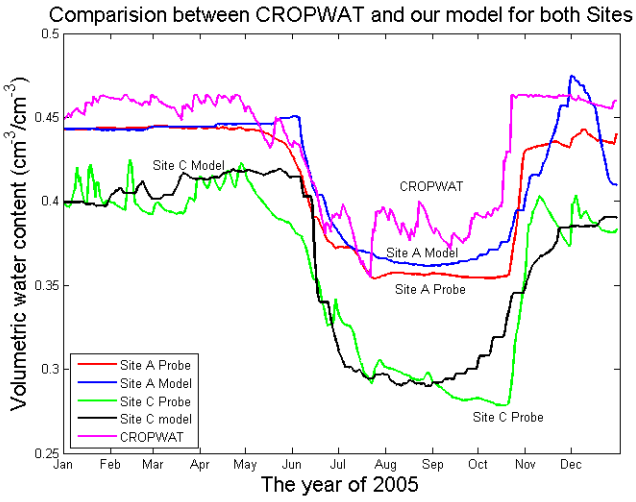

Figure 8: The comparison between the Penman-Monteith / CROPWAT model, the validated Roose and Fowler model and the measured TDR data.

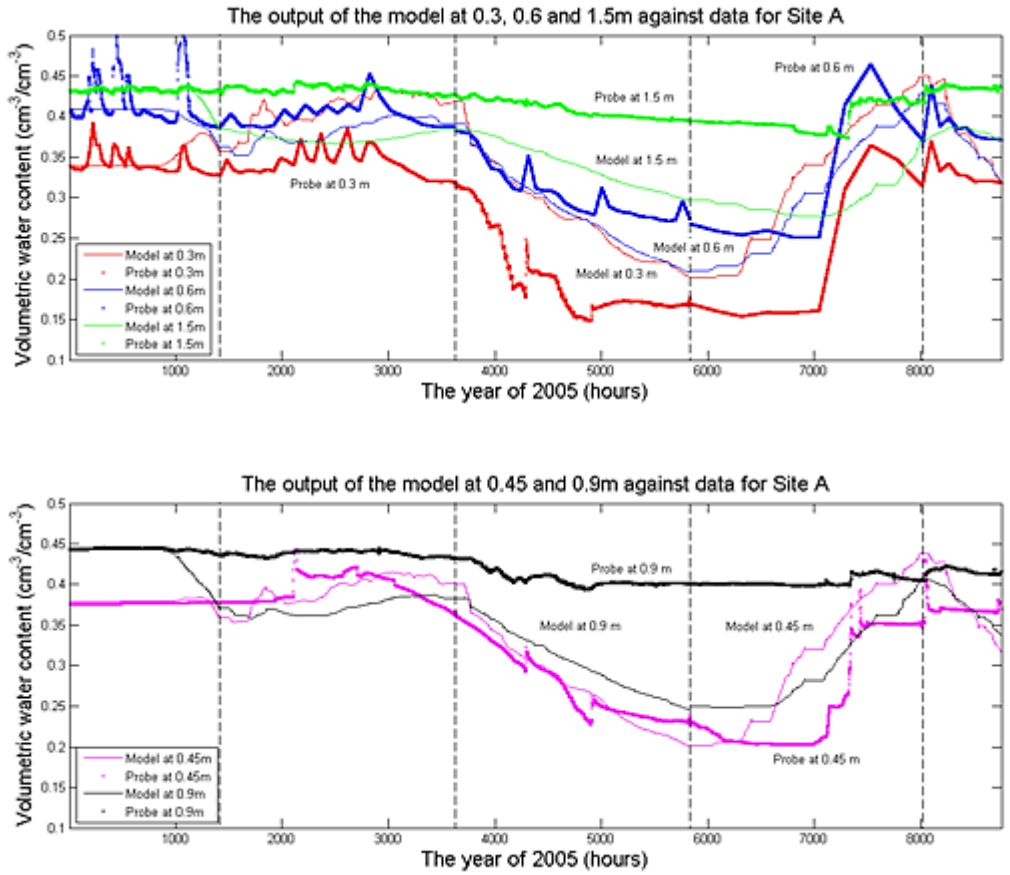

Figure 9: The model fittings for 2005 for location A for constant values of m and k_s.

Tables

Variables	Range	Units
δ	0 to 5x10^{-3}	-
α_1	0 to 5x10^{-6}	ms^{-1} of water
α_2	0 to 2.5x10^{-11}	ms^{-1} of water
α_3	0 to 1.25x10^{-16}	ms^{-1} of water
β_1	0 to 5x10^{-5}	ms^{-1} of water/$degC$
β_2	0 to 2.5x10^{-9}	ms^{-1} of water/$degC^2$
β_3	0 to 1.25x10^{-13}	ms^{-1} of water/$degC^3$
γ_1	0 to 2.5x10^{-3}	ms^{-1} of water/$ms^{-1}$of air
γ_2	0 to 6.25x10^{-6}	ms^{-1} of water/$m^2s^{-2}$of air
γ_3	0 to 1.5625x10^{-8}	ms^{-1} of water/$m^3s^{-3}$of air
λ_1	-5x10^{-3} to 5x10^{-3}	Pa
λ_2	-1.5x10^{-3} to 1.5x10^{-3}	$Pa/\ \%humidity$
λ_3	-0.25 to 0.25	$Pa/\ degC$
c	0 to 2.5x10^{-3}	ms^{-1} of water
m	0.1 to 0.5	-
k_r	0 to 2.5x10^{-4}	$ms^{-1}Pa$
k_z	0 to 4.6x10^{-11}	$m^4s^{-1}Pa^{-1}$
Fixed values	**Value**	**Units**
ϕ	0.4	-
ρ	2.6x10^3	$kg\ m^{-3}$
p_c	0.232x10^5	Pa
D_0	1.1574x10^{-6}	m^2s^{-1}
k_s	5.78x10^{-9} to 5.78x10^{-8}	m^2
a	5x10^{-4}	m

l_d	1.785×10^3	m of roots per m^3 of soil
L	0.8	m

Table 1: A list of variables and fixed values used within the model

Inputs	**Outputs**
Water flux at the top of the soil	Water uptake by root system
Root parameters	Water saturations levels over time for any given depth up to 2 meters
Soil parameters	

Table 2: Inputs and outputs for the model

Location	A				C			
Season	**Winter**	**Spring**	**Summer**	**Autumn**	**Winter**	**Spring**	**Summer**	**Autumn**
2005 Linear W, SOS	5.79	6.45	17.30	19.94	0.28	0.65	4.07	4.52
2005 Non-linear W, SOS	3.77	4.70	15.07	16.62	2.08	0.39	2.57	3.31
2006 Non-linear W, SOS	22.23	8.91	26.79	18.78	1.72	1.28	3.94	9.77

Table 3: The sum of square results for linear and non-linear W, for different measurement locations and seasons: fitted results for 2005 and forecast model run results for 2006.